VASP: Hybrid functionals

University of Vienna,
Faculty of Physics and Center for Computational Materials Science,
Vienna, Austria

universität wien

Outline

- Introduction: DFT, HF
- Hybrid functionals
- Assessing hybrid functionals
- Returning to direct optimization

The Many-Body Schrödinger equation

$$\hat{H}\Psi(\mathbf{r}_1,...,\mathbf{r}_N) = E\Psi(\mathbf{r}_1,...,\mathbf{r}_N)$$

$$\left(-\frac{1}{2}\sum_i \Delta_i + \sum_i V(\mathbf{r}_i) + \sum_{i\neq j}\frac{1}{|\mathbf{r}_i-\mathbf{r}_j|}\right)\Psi(\mathbf{r}_1,...,\mathbf{r}_N) = E\Psi(\mathbf{r}_1,...,\mathbf{r}_N)$$

For instance, many-body WF storage demands are prohibitive:

$\Psi(\mathbf{r}_1,...,\mathbf{r}_N)$ $(\#\text{grid points})^N$

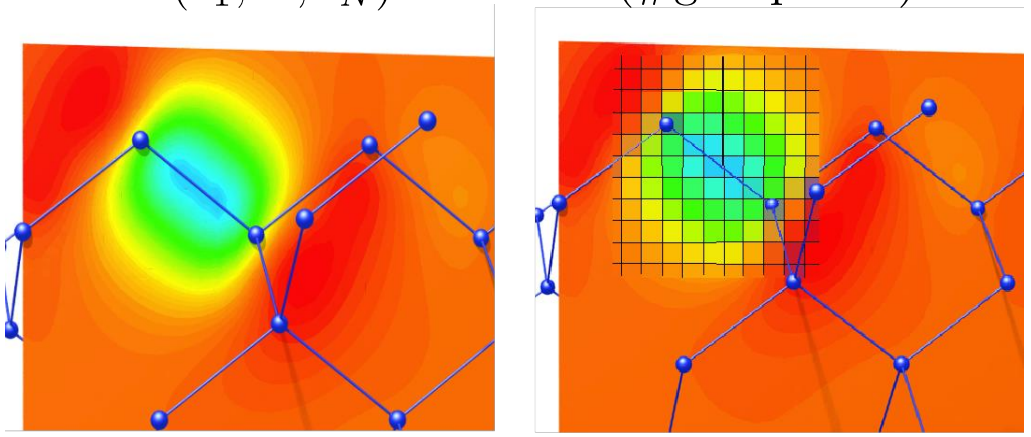

5 electrons on a 10×10×10 grid ~ 10 PetaBytes !

A solution: map onto “one-electron” theory:

$$\Psi(\mathbf{r}_1,...,\mathbf{r}_N) \rightarrow \{\psi_1(\mathbf{r}),\psi_2(\mathbf{r}),...,\psi_N(\mathbf{r})\}$$

Hohenberg-Kohn-Sham DFT

Map onto "one-electron" theory:

$$\Psi(\mathbf{r}_1, ..., \mathbf{r}_N) \rightarrow \{\psi_1(\mathbf{r}), \psi_2(\mathbf{r}), ..., \psi_N(\mathbf{r})\} \qquad \Psi(\mathbf{r}_1, ..., \mathbf{r}_N) = \prod_i^N \psi_i(\mathbf{r}_i)$$

Total energy is a functional of the density:

$$E[\rho] = T_s[\{\psi_i[\rho]\}] + E_H[\rho] + E_{\mathrm{xc}}[\rho] + E_Z[\rho] + U[Z]$$

The density is computed using the one-electron orbitals:

$$\rho(\mathbf{r}) = \sum_i^N |\psi_i(\mathbf{r})|^2$$

The one-electron orbitals are the solutions of the Kohn-Sham equation:

$$\left(-\frac{1}{2}\Delta + V_Z(\mathbf{r}) + V_H[\rho](\mathbf{r}) + V_{\mathrm{xc}}[\rho](\mathbf{r})\right)\psi_i(\mathbf{r}) = \epsilon_i \psi_i(\mathbf{r})$$

BUT: $E_{\mathrm{xc}}[\rho] = ???$ $\quad V_{\mathrm{xc}}[\rho](\mathbf{r}) = ???$ $\quad E_{\mathrm{xc}} = E - T_s - E_H - E_{\mathrm{ext}}$

In practice: Exchange-correlation functionals are modeled on the uniform electron gas (Monte Carlo calculations): *e.g.* the Local Density Approximation (LDA).

Hartree-Fock

Slater determinant

$$\Psi(\mathbf{r}_1,...,\mathbf{r}_N) = \frac{1}{\sqrt{N!}} \begin{vmatrix} \psi_1(\mathbf{r}_1) & \psi_1(\mathbf{r}_1) & \cdots & \psi_N(\mathbf{r}_1) \\ \psi_1(\mathbf{r}_2) & \psi_2(\mathbf{r}_2) & \cdots & \psi_N(\mathbf{r}_2) \\ \vdots & \vdots & & \vdots \\ \psi_1(\mathbf{r}_N) & \psi_2(\mathbf{r}_N) & \cdots & \psi_N(\mathbf{r}_N) \end{vmatrix}$$

For instance

$$\Psi(\mathbf{r}_1,\mathbf{r}_2) = \frac{1}{\sqrt{2}}\Big(\psi_1(\mathbf{r}_1)\psi_2(\mathbf{r}_2) - \psi_1(\mathbf{r}_2)\psi_2(\mathbf{r}_1)\Big)$$

Pauli exclusion principle:

$$\psi_1 = \psi_2 \Rightarrow \Psi(\mathbf{r}_1,\mathbf{r}_2) = 0$$

Roothaan equations:

$$\Big(-\frac{1}{2}\Delta + V_Z(\mathbf{r}) + V_H[n](\mathbf{r})\Big)\psi_i(\mathbf{r}) + \int V_X(\mathbf{r},\mathbf{r}')\psi_i(\mathbf{r}')d\mathbf{r}' = \epsilon_i\psi_i(\mathbf{r})$$

Orbital dependent non-local potential

$$V_X(\mathbf{r},\mathbf{r}') = -\sum_j^N \frac{\psi_j(\mathbf{r})\psi_j^*(\mathbf{r}')}{|\mathbf{r}-\mathbf{r}'|}$$

Compare to DFT:

$$V_{\mathrm{xc}}[\rho](\mathbf{r})\psi_i(\mathbf{r})$$

$$E_{\mathrm{HF}} = \langle\Psi|H|\Psi\rangle = \sum_i^N \epsilon_i - \frac{1}{2}\langle\Psi|\hat{V}_{\mathrm{H}} + \hat{V}_{\mathrm{X}}|\Psi\rangle$$

Per definition: no electronic correlation

Need to go beyond Hartree-Fock?

Simplest possible metal: Homogeneous electron gas

HF for the homogeneous electron gas:

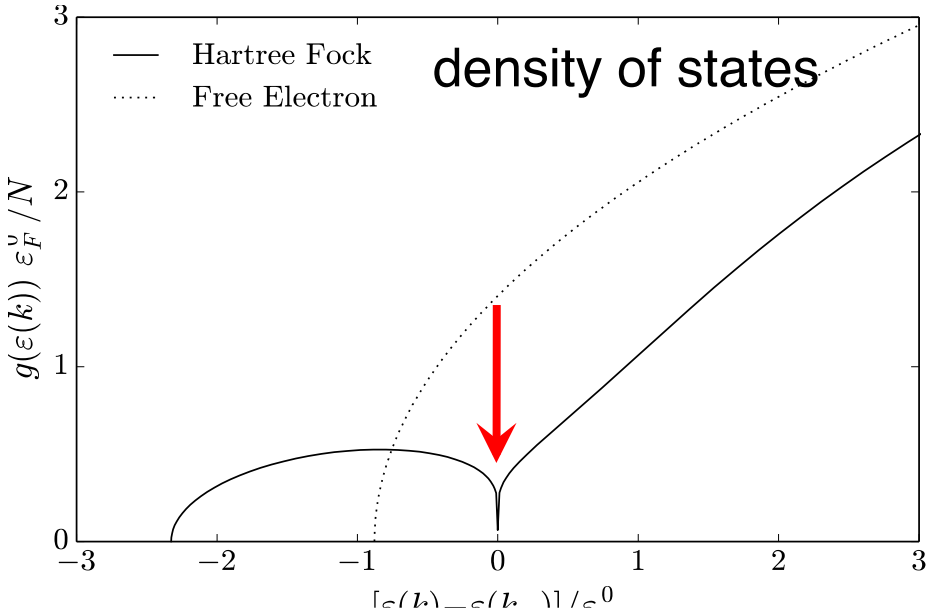

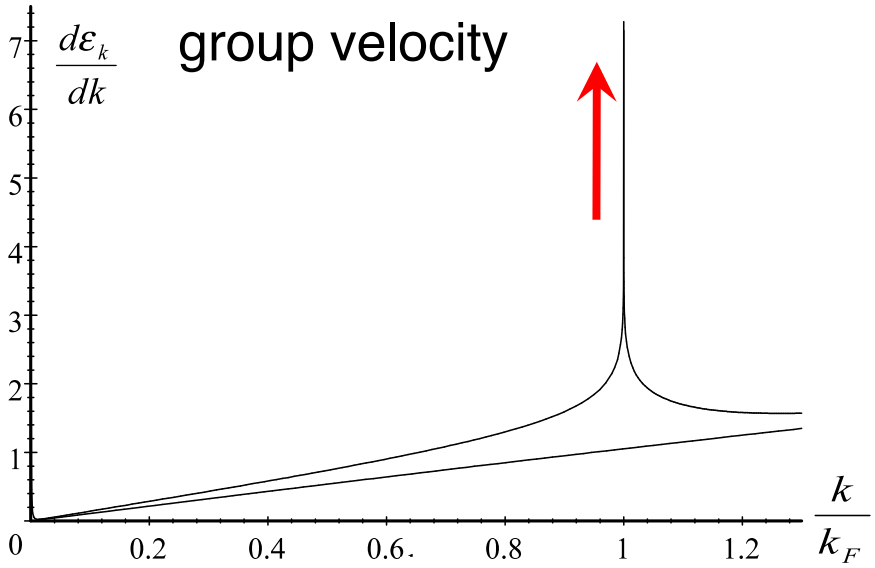

G. Brocks, AQM lecture notes 2004

At the Fermi energy: - DoS -> 0

- v_g -> infinity

Problem: $\frac{1}{|\mathbf{r}-\mathbf{r}'|}$ FT $\frac{4\pi}{\mathbf{q}^2}$

Singularity for $\mathbf{q}=0$

Solution: introduce screening

HEG exact in PBE0 and HSE03, not B3LYP

J. Paier, , M. Marsman, and G. Kresse, J. Chem. Phys. **127**, 024103 2007

Need to go beyond DFT and Hartree-Fock?

Lattice constants and Bulk moduli:
AlP, AlAs, BAs, BP, Si, C, SiC, MgO, LiF

	LDA		PBE		HF	
	Δa_0	ΔB_0	Δa_0	ΔB_0	Δa_0	ΔB_0
MRE	-1.4	3.5	0.8	-7.2	0.4	8.2
MARE	1.4	7.9	0.8	7.2	0.7	8.2

(All in %)

Atomization energy

	LDA	PBE
MRE (%)	17.3	-1.9
MARE (%)	17.3	3.4
ME (eV)	0.76	0.14

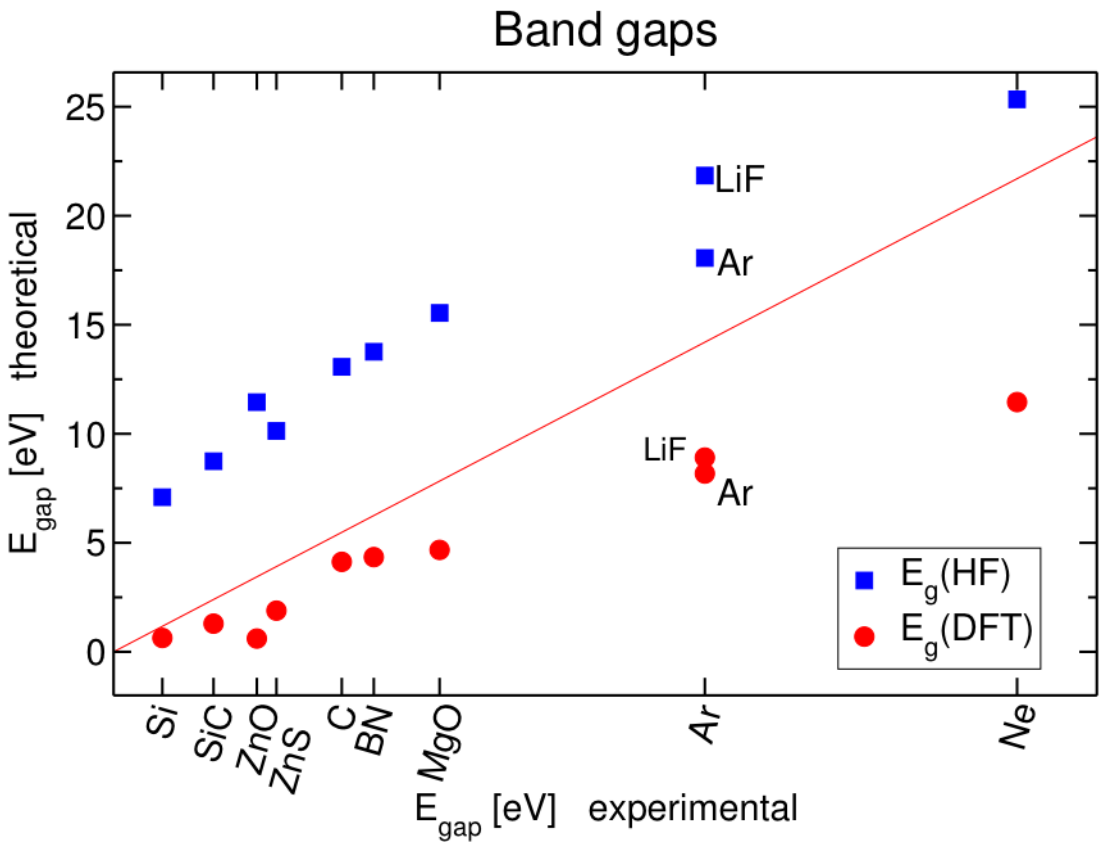

(More) accurate treatment of electronic correlation needed for, e.g:

- Band gaps (optical properties
- Total energy differences with chemical accuracy
  (1 kcal/mol ≈ 40 meV)
- Atomization and formation energies
- Reaction barriers
- Van der Waals interactions

Hartree-Fock/DFT hybrid functionals

Definition: Exchange-correlation functionals that admix a certain amount of Fock exchange to (a part of) a local or semi-local density functional.

- Present a definite improvement over the (semi)-local density functional description of the properties of molecular systems.
- Some hybrid functionals yield an improved description of structural, electronic, and thermo-chemical properties of small/medium gap solid state systems.

Hybrid functionals: PBE0, HSE

PBE0:

$$E_{xc}^{\mathrm{PBE0}} = \frac{1}{4} E_x^{\mathrm{HF}} + \frac{3}{4} E_x^{\mathrm{PBE}} + E_c^{\mathrm{PBE}}$$

non-empirical: justified using the adibatic connection formula.

J. Perdew, M. Ernzerhof, and K. Burke, J. Chem. Phys. 105, 9982 (1996).

HSE03:

$$E_{\mathrm{xc}}^{\mathrm{HSE03}} = \frac{1}{4} E_{\mathrm{x}}^{\mathrm{HF,SR}}(\mu) + \frac{3}{4} E_{\mathrm{x}}^{\mathrm{PBE,SR}}(\mu) + E_{\mathrm{x}}^{\mathrm{PBE,LR}}(\mu) + E_{\mathrm{c}}^{\mathrm{PBE}}$$

Decomposed Coulomb kernel (Savin *et al.*):

$$\frac{1}{r} = S_\mu(r) + L_\mu(r) = \frac{\mathrm{erfc}(\mu r)}{r} + \frac{\mathrm{erf}(\mu r)}{r}$$

semiemperical: μ is chosen to yield an optimal description of the atomization energies of the molecues in Pople's G2-1 test set.

J. Heyd, G. E. Scuseria, and M. Ernzerhof, J. Chem. Phys. 118, 8207 (2003).

Hybrid functionals: B3LYP

B3LYP:

$$E_{\mathrm{X}}^{\mathrm{B3LYP}} = 0.8E_{\mathrm{X}}^{\mathrm{LDA}} + 0.2E_{\mathrm{X}}^{\mathrm{HF}} + 0.72\Delta E_{\mathrm{X}}^{\mathrm{B88}}$$
$$E_{\mathrm{C}}^{\mathrm{B3LYP}} = 0.19E_{\mathrm{C}}^{\mathrm{VWN3}} + 0.81E_{\mathrm{C}}^{\mathrm{LYP}}$$

semiempirical: coefficients chosen to reproduce experimental atomization energies, electron and proton affinities and ionization potentials of the molecules in Pople's G2 test set and their atomic constituents.

A. D. Becke, J. Chem. Phys. 98, 5648 (1993).
M. J. Frisch et al., GAUSSIAN03 Rev. C.02, Gaussian Inc., Wallingford, CT 2004.

Computational aspects

$$E_x^{\mathrm{HF}} \propto \sum_{\mathbf{k}n,\mathbf{q}m} \int\int d^3\mathbf{r} d^3\mathbf{r}' \psi^*_{\mathbf{k}n}(\mathbf{r}) \psi_{\mathbf{q}m}(\mathbf{r}) K(\mathbf{r},\mathbf{r}') \psi^*_{\mathbf{q}m}(\mathbf{r}') \psi_{\mathbf{k}n}(\mathbf{r}')$$

with

$$K(\mathbf{r},\mathbf{r}') = \frac{1}{|\mathbf{r}-\mathbf{r}'|} \quad \text{or} \quad \frac{\mathrm{erfc}(\mu|\mathbf{r}-\mathbf{r}'|)}{|\mathbf{r}-\mathbf{r}'|}$$

- FFT overlap density to reciprocal space

$$\rho(\mathbf{G}) = \mathrm{FFT}\{\psi^*_{\mathbf{q}m}(\mathbf{r}')\psi_{\mathbf{k}n}(\mathbf{r}')\}$$

- Division by Laplace operator and FFT to real space

$$V(\mathbf{G}) = \frac{4\pi e^2}{|\mathbf{G}|^2}\rho(\mathbf{G}) \qquad V(\mathbf{r}) = \mathrm{FFT}\{V(\mathbf{G})\}$$

- Evaluate

$$\int \psi^*_{\mathbf{k}n}(\mathbf{r})\psi_{\mathbf{q}m}(\mathbf{r})V(\mathbf{r})d^3\mathbf{r}$$

N.B.: for all combinations of **k**, **q**, *n*, and *m*.

Computational aspects: Scaling

$$E_x^{\mathrm{HF}} \propto \sum_{\mathbf{k}n,\mathbf{q}m} \int\int d^3\mathbf{r} d^3\mathbf{r}' \psi^*_{\mathbf{k}n}(\mathbf{r}) \psi_{\mathbf{q}m}(\mathbf{r}) K(\mathbf{r},\mathbf{r}') \psi^*_{\mathbf{q}m}(\mathbf{r}') \psi_{\mathbf{k}n}(\mathbf{r}')$$

Effort:

$$(N_{\mathrm{bands}} \times N_{\mathrm{k}})(N_{\mathrm{bands}} \times N_{\mathrm{q}}) \times N_{\mathrm{FFT}} \ln N_{\mathrm{FFT}}$$

- Bulk: $N_{\mathrm{bands}} \propto N_{\mathrm{atoms}} \quad N_{\mathrm{k}} \propto 1/N_{\mathrm{atoms}}$

$$\Rightarrow \; N_{\mathrm{FFT}} \ln N_{\mathrm{FFT}} \propto N_{\mathrm{atoms}}$$

- Molecular systems: $N_{\mathrm{k}} = 1$

$$\Rightarrow \; N_{\mathrm{bands}} \times N_{\mathrm{bands}} \times N_{\mathrm{FFT}} \ln N_{\mathrm{FFT}} \propto N_{\mathrm{atoms}}^3$$

Computational aspects: Downsampling

Convergence of E_X^{HF} w.r.t. the BZ sampling use to represent V_X^{HF}

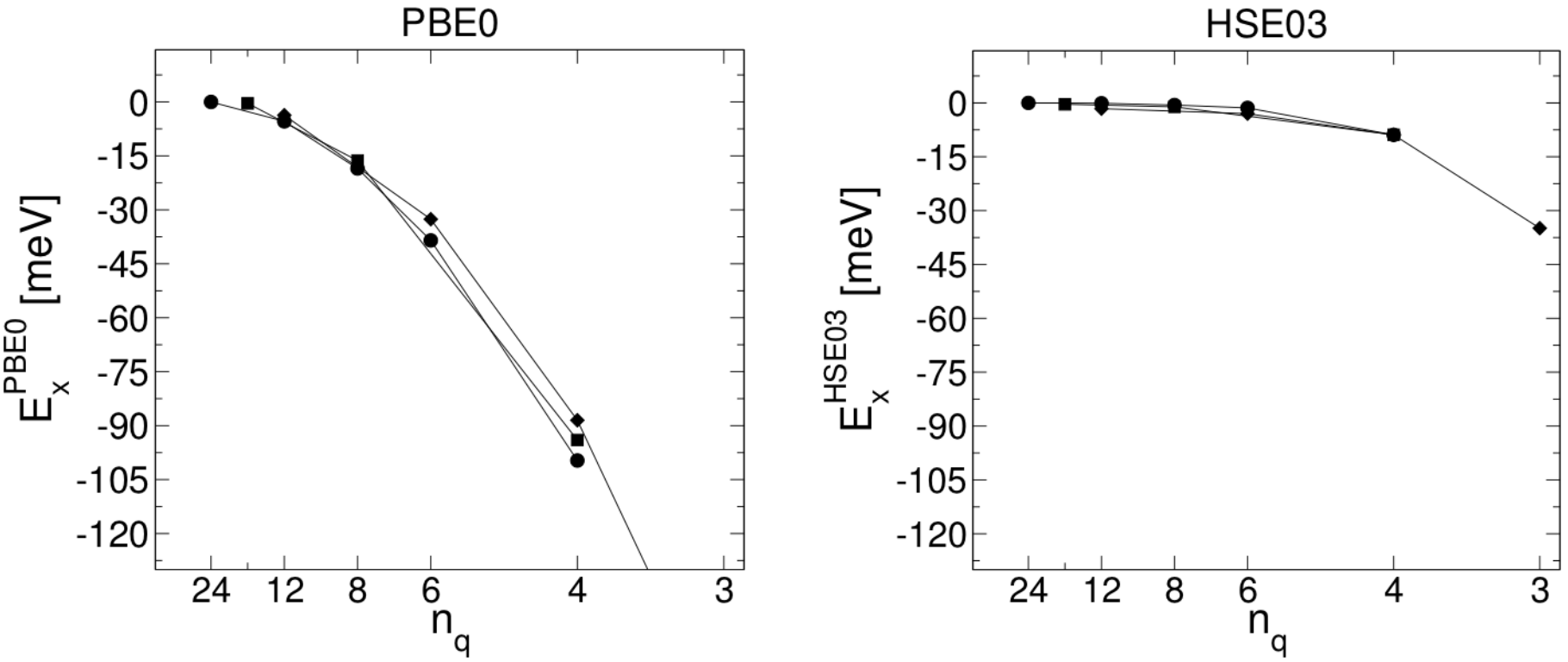

Example: Al (fcc)

Short(er) range in real space $\Longrightarrow$ Reduced BZ sampling

Downsampling (cont.)

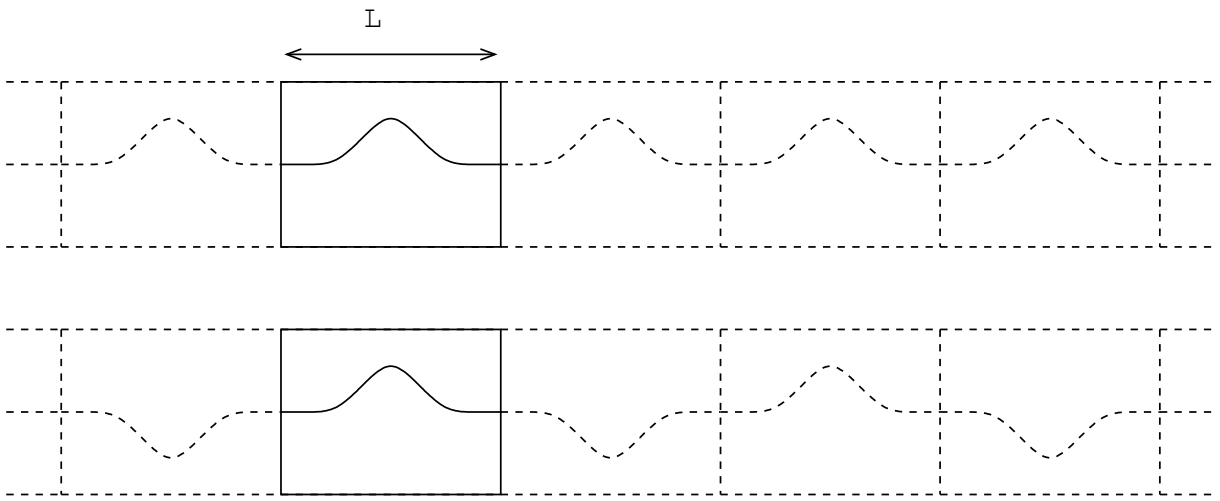

1 band
2 **k**-points

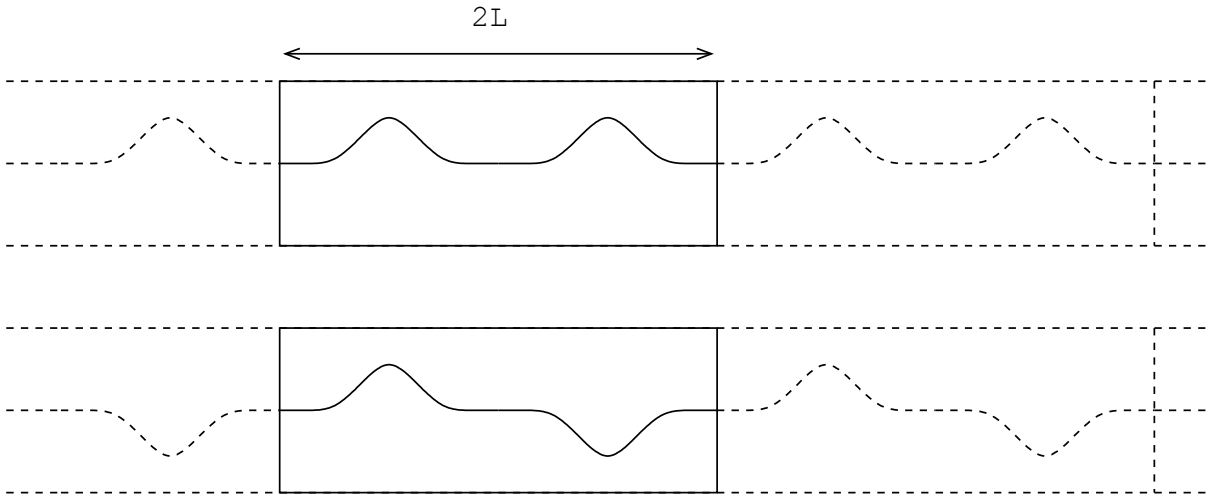

2 bands
1 **k**-point

Unit cells		**k**-points
1	⇔	*n*
n		1

Downsampling (cont.)

Unit cells		**k**-points
1	⇔	*n*
n		1

Assume a maximum interaction range $R = mL$, then a supercell of twice this size, i.e., $2m$ unit cells, correctly incorporates all interactions using only the gamma-point.

This is equivalent to the description one obtains using a single unit cell and an equidistant $2m$ sampling of the 1st BZ.

Ergo: reducing the range of the Fock exchange interaction in the HSE functional allows for the representation of the Fock potential on a coarser grid of **k**-points.

Down-sampling (cont.)

The HSE Fock exchange energy:

$$E_{\mathrm{x}}^{\mathrm{SR}}(\mu) = -\frac{e^2}{2}\sum_{\mathbf{k}n,\mathbf{q}m} 2w_{\mathbf{k}}2w_{\mathbf{q}}f_{\mathbf{k}n}f_{\mathbf{q}m} \times \iint d^3\mathbf{r}d^3\mathbf{r}'\frac{\mathrm{erfc}(\mu|\mathbf{r}-\mathbf{r}'|)}{|\mathbf{r}-\mathbf{r}'|}\phi^*_{\mathbf{k}n}(\mathbf{r})\phi_{\mathbf{q}m}(\mathbf{r})\phi^*_{\mathbf{q}m}(\mathbf{r}')\phi_{\mathbf{k}n}(\mathbf{r}').$$

The representation of the corresponding short-range Fock potential in reciprocal space:

$$V_{\mathbf{k}}^{\mathrm{SR}}(\mathbf{G},\mathbf{G}') = \langle \mathbf{k}+\mathbf{G}|V_x^{\mathrm{SR}}[\mu]|\mathbf{k}+\mathbf{G}'\rangle = -\frac{4\pi e^2}{\Omega}\sum_{m\mathbf{q}} 2w_{\mathbf{q}}f_{\mathbf{q}m}\sum_{\mathbf{G}''}\frac{C^*_{\mathbf{q}m}(\mathbf{G}'-\mathbf{G}'')C_{\mathbf{q}m}(\mathbf{G}-\mathbf{G}'')}{|\mathbf{k}-\mathbf{q}+\mathbf{G}''|^2} \times \left(1-e^{-|\mathbf{k}-\mathbf{q}+\mathbf{G}''|^2/4\mu^2}\right).$$

Full **q**-grid:

$$\{\mathbf{q}\} = \{\frac{m_1}{N_1}\mathbf{b}_1 + \frac{m_2}{N_2}\mathbf{b}_2 + \frac{m_3}{N_3}\mathbf{b}_3 | m_i = 0, ..., N_i - 1\}$$

Downsampled **q**-grid:

$$\{\mathbf{q}\}_{\mathbf{k}} = \{\mathbf{k} + \sum_{i=1}^{3} m_i \frac{C_i}{N_i}\mathbf{b}_i | m_i = 0, ..., \frac{N_i}{C_i} - 1\}$$

Atomization energies of small molecules

Subset of G2-1 test set: Deviation w.r.t. experiment, in [kcal/mol]

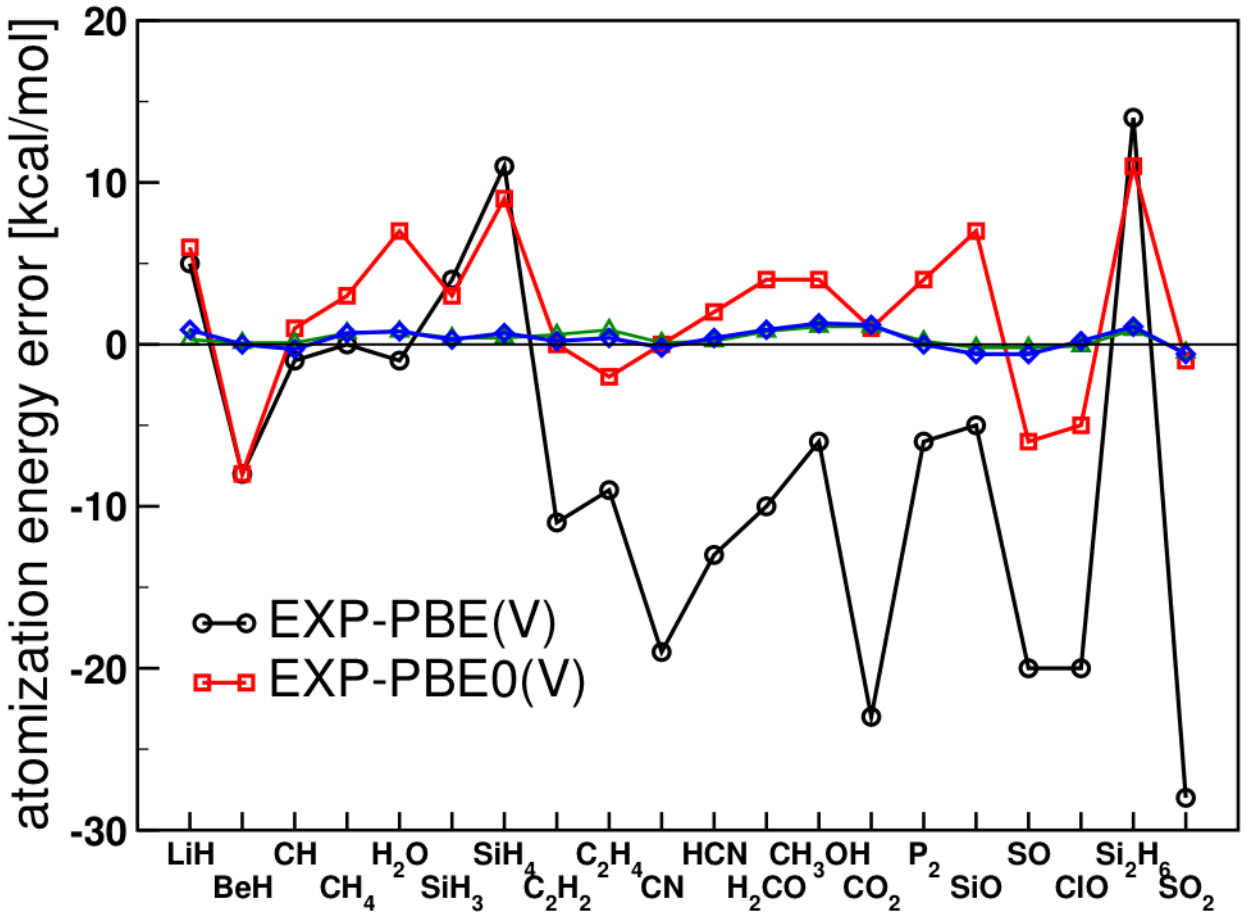

Significant improvement of atomization energies

Lattice constants: PBE, PBE0, HSE03, and B3LYP

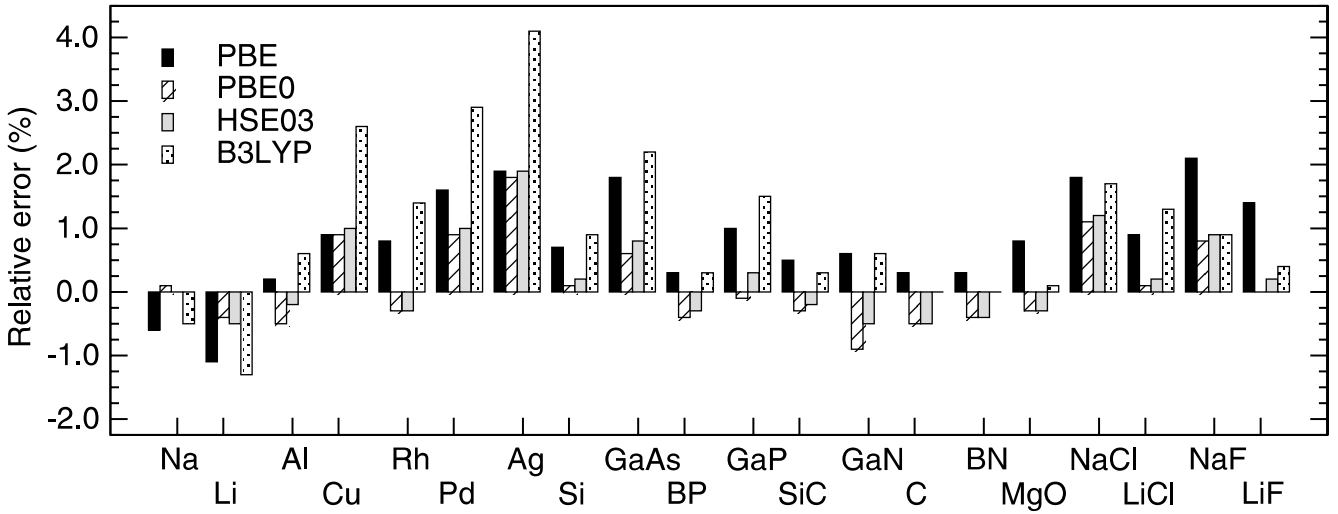

Relative error in the PBE, PBE0, HSE03, and B3LYP lattice constants with respect to experiment.

MRE: Mean relative error (%)
MARE: Mean absolute relative error

M. Marsman, *et al.*,
J. Phys. Cond. Matt. 20 (2008) 064201

Lattice constant		
	MRE	MARE
PBE	0.8	1.0
PBE0	0.1	0.5
HSE	0.2	0.5
B3LYP	1.0	1.2

Bulk modulus		
	MRE	MARE
PBE	-9.8	9.4
PBE0	-1.2	5.7
HSE	-3.1	6.4
B3LYP	-10.2	11.4

Solid state systems: Atomization energies

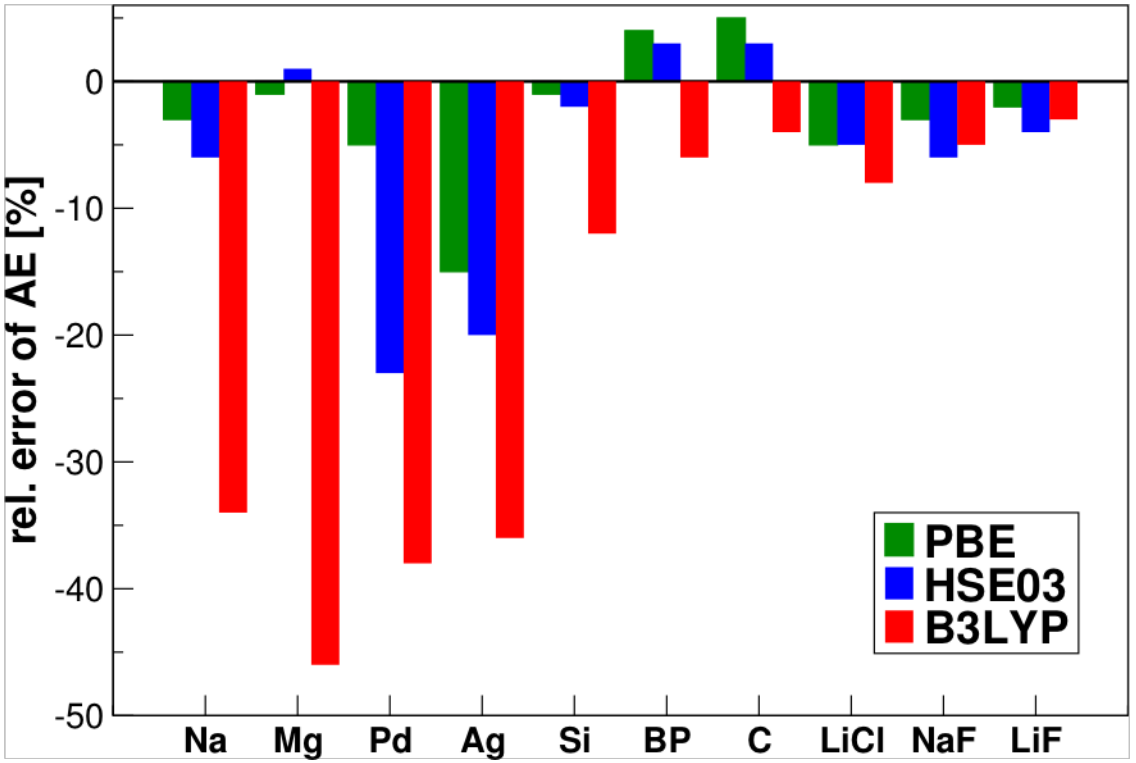

	PBE	PBE0	HSE03	B3LYP
ME	−0.045	−0.228	−0.184	−0.590
MAE	0.134	0.286	0.252	0.590

(in eV/atom)

Solid state systems: Atomization energies

- Hybrid functionals overestimate the exchange splitting in *d*-elements: leads to an increased stability of the spin-polarized atom.
- B3LYP overestimates E_{xc} of localized electrons.
- B3LYP fails to describe "free electron like" behaviour:
  LYP underestimates the correlation energy in itinerant systems
  (does not attain HEG limit!).

J. Paier, M. Marsman, and G. Kresse, J. Chem. Phys. 127, 024103 (2007).

Solid state systems: Heats of formation

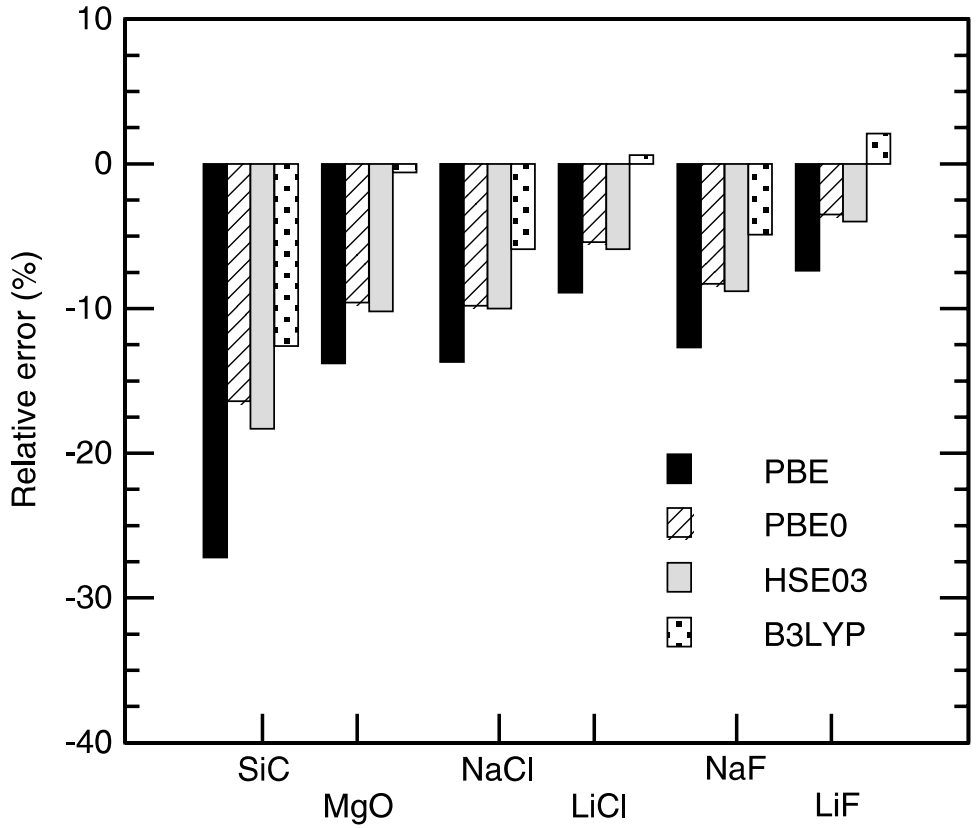

Figure 7. Relative error in the PBE, PBE0, HSE03, and B3LYP heats of formation with respect to experiment.

M. Marsman, J. Paier, A. Stroppa and G. Kresse, J. Phys. Cond. Matt. 20 (2008) 064201

Solid state systems: Band gaps

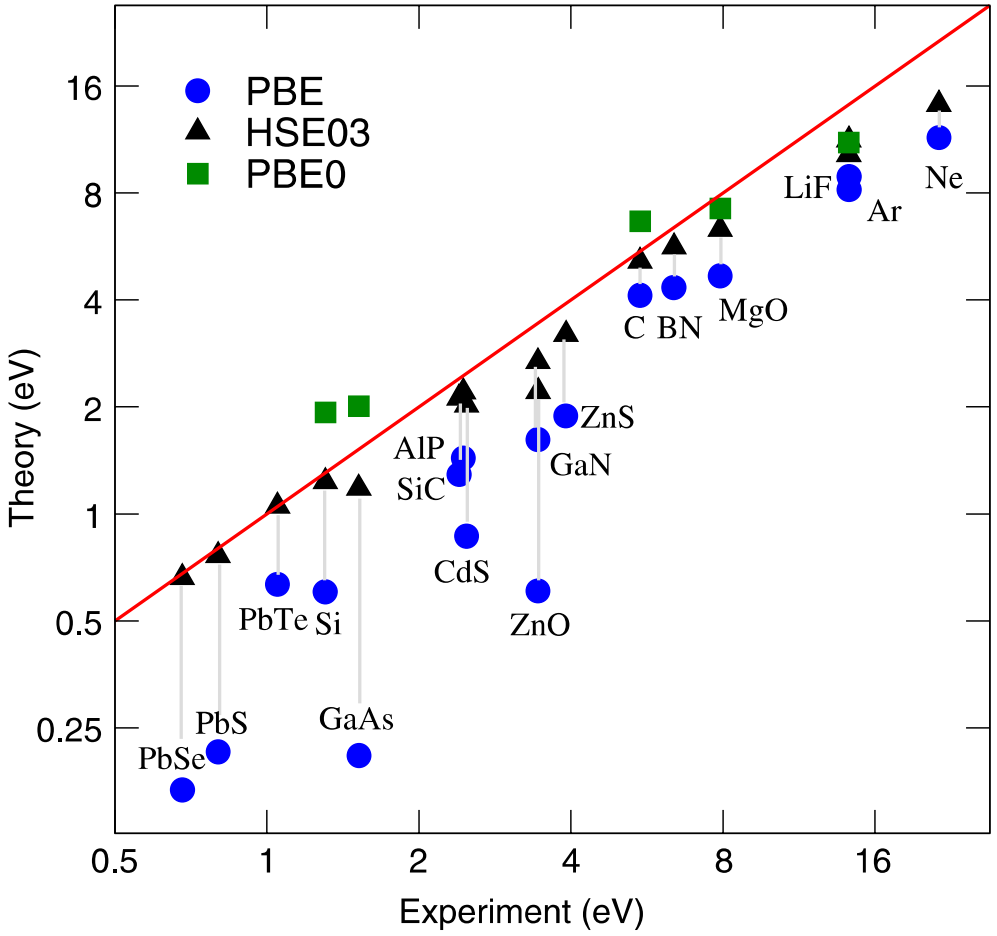

Figure 8. Band gaps from PBE, PBE0, and HSE03 calculations, plotted against data from experiment.

M. Marsman, J. Paier, A. Stroppa and G. Kresse, J. Phys. Cond. Matt. 20 (2008) 064201

Transition-metal monoxides: MnO

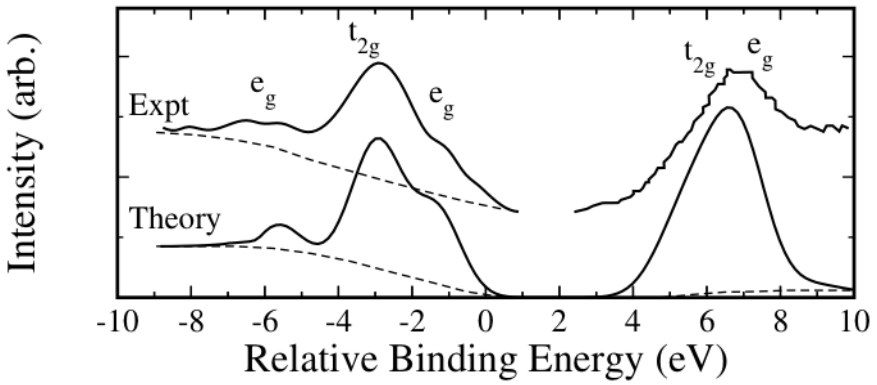

Comparison between PBE0 d-projected DOS (bottom) of both Mn sites, together with the experimental (top) inverse photoemission data, and the difference between on- and off-resonance photo-Emission spectra.

C. Franchini, V. Bayer, R. Podloucky, J. Paier, and G. Kresse, Phys. Rev. B 72, 045132 (2005).

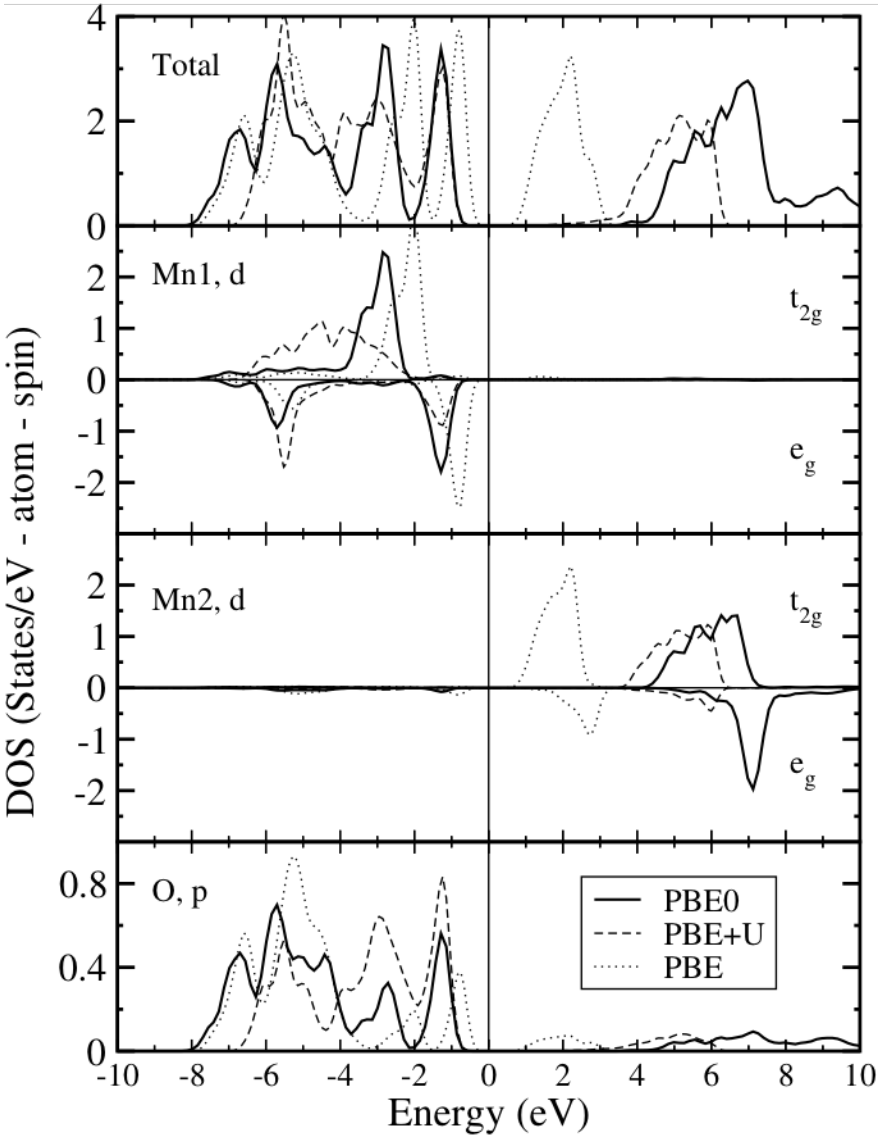

Transition-metal monoxides (cont.)

Lattice constant

Magnetic moment

Band gap

		a_0 (Å)	M_s (μ_B)	Δ (eV)
MnO	LDA	4.31	4.14	0.4
	HSE03	4.44	4.52	2.8
	exp.	4.45	4.58	3.9
FeO	LDA	4.17	3.26	-
	HSE03	4.33	3.63	2.2
	exp.	4.33	3.32/4.2	2.4
CoO	LDA	4.10	2.23	-
	HSE03	4.26	2.67	3.4
	exp.	4.25	3.35/4.0	2.5
NiO	LDA	4.06	1.06	0.4
	HSE03	4.18	1.65	4.2
	exp.	4.17	1.64	4.0

CO adsorption on d-metal surfaces

- DFT incorrectly predicts that CO prefers the hollow site: P. Feibelman *et al.*, J. Phys. Chem. B 105, 4018 (2001)
- The error is relatively large. Best DFT/PBE calculations:

  CO@Cu(111): -170 meV
  CO@Rh(111): -40 meV
  CO@Pt(111): -100 meV

- 4 layers, $c(2 \times 4), \Theta = 0.25$ ML, asymmetric setup, 10 Å vacuum.

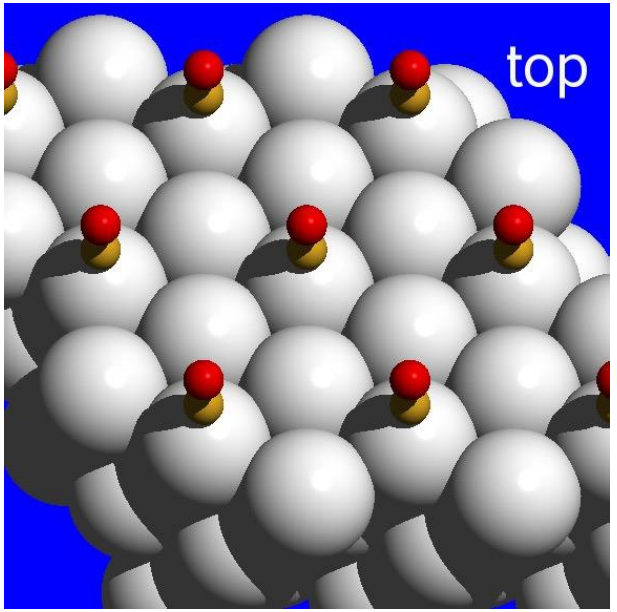

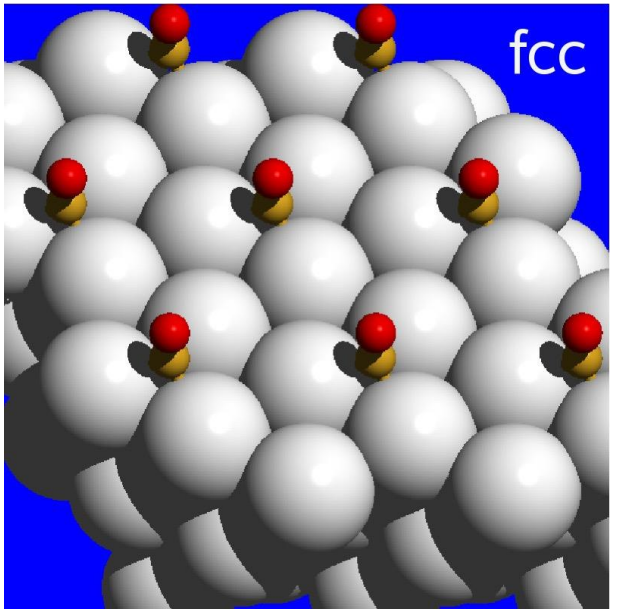

CO adsorption on d-metal surfaces (cont. I)

CO @		top	fcc	hcp	Δ
Cu(111)	PBE	0.709	0.874	0.862	−0.165
	PBE0	0.606	0.579	0.565	0.027
	HSE03	0.561	0.555	0.535	0.006
	exp.	0.46-0.52			
Rh(111)	PBE	1.870	1.906	1.969	−0.099
	PBE0	2.109	2.024	2.104	0.005
	HSE03	2.012	1.913	1.996	0.016
	exp.	1.43-1.65			
Pt(111)	PBE	1.659	1.816	1.750	−0.157
	PBE0	1.941	1.997	1.944	−0.056
	HSE03	1.793	1.862	1.808	−0.069
	exp.	1.43-1.71			

CO adsorption on d-metal surfaces (cont. II)

Hybrid functionals reduce the tendency to stabilize adsorption at the hollow sites w.r.t. the top site.

Reduced CO $2\pi^*$ $\leftrightarrow$ metal-*d* interaction

- Improved description of the CO LUMO ($2\pi^*$) w.r.t. the Fermi level (shifted upwards).
- Downshift of the metal d-band center of gravity in Cu(111).
- But: Overestimation of the metal d-bandwidth.

A. Stroppa, K. Termentzidis, J. Paier, G. Kresse, and J. Hafner, Phys. Rev. B 76, 195440 (2007).
A. Stroppa and G. Kresse, New Journal of Physics 10, 063020 (2008).

Conclusions

$$E_{\mathrm{xc}}^{\mathrm{hyb.}} = aE_X^{\mathrm{HF}} + (1-a)E_X^{\mathrm{DFT}} + E_c^{\mathrm{DFT}}$$

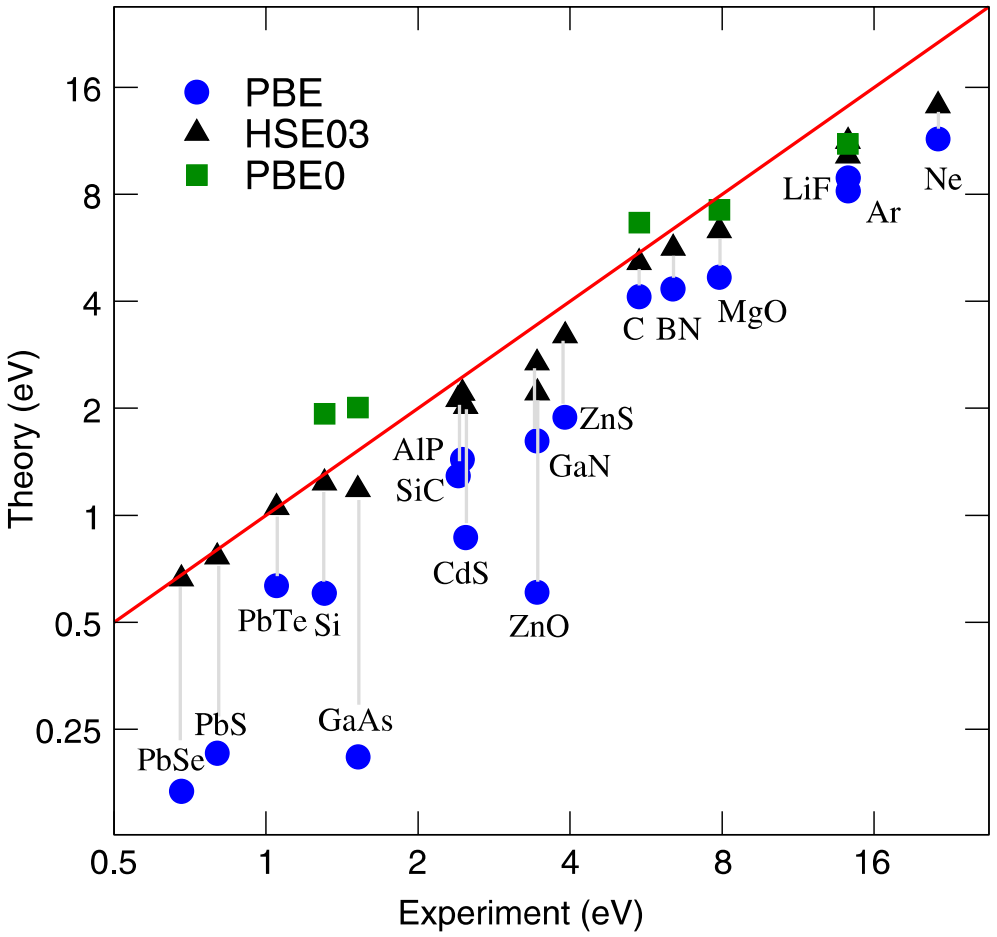

Figure 8. Band gaps from PBE, PBE0, and HSE03 calculations, plotted against data from experiment.

Lattice constant

	MRE	MARE
PBE	0.8	1.0
PBE0	0.1	0.5
HSE	0.2	0.5
B3LYP	1.0	1.2

Bulk modulus

	MRE	MARE
PBE	-9.8	9.4
PBE0	-1.2	5.7
HSE	-3.1	6.4
B3LYP	-10.2	11.4

Atomization energy

	MRE	MARE
PBE	-1.9	3.4
PBE0	-6.5	7.4
HSE	-5.1	6.3
B3LYP	-17.6	17.6

M. Marsman, J. Paier, A. Stroppa and G. Kresse, J. Phys. Cond. Matt. 20 (2008) 064201

Conclusions (cont.)

Solid state systems:

- The PBE0 and HSE hybrid functionals provide an improved description of the structural (lattice constants and bulk moduli) and electronic (band gap) properties of systems with a small/medium sized band gap.

- PBE0, HSE, and B3LYP atomization energies are in overall worse agreement with experiment than those obtained using the semi-local PBE density functional, in case of B3LYP even drastically so.
  This is mainly due to a worse description of metallic systems.

- CO adsorption on *d*-metal (111) surfaces: hybrid functionals reduce the tendency to stabilize adsorption at the hollow sites w.r.t. the top site.

INCAR Tags and links

Hybrid functionals and Hartree-Fock
The VASP manual chapter on hybrid functionals and Hartree-Fock.

LHFCALC	Switch on Hybrid and Hartree-Fock type calculations.
HFSCREEN	Specifies the range separating parameter in HSE functionals.
ENCUTFOCK	Specifies the FFT grids used in the HF routines.
GGA-tag	Override the type of density functional specified in the POTCAR.
NKRED, NKREDX, NKREDY, NKREDZ	Down-sampling the k-point mesh in the representation of the Fock potential.
AEXX, AGGAX, AGGAC and ALDAC	The fractions of Fock-exchange, gradient corrections to the exchange and correlation, and the fraction of LDA correlation.

INCAR settings:

PBE0: LHFCALC = .TRUE.
HSE06:† LHFCALC = .TRUE. ; HFSCREEN = 0.2 (with PBE POTCAR, or GGA = PE).
B3LYP: LHFCALC = .TRUE. ; GGA = B3 ; AEXX = 0.2 ; AGGAX = 0.72 ; AGGAC = 0.81 ; ALDAC = 0.19
Hartree-Fock: LHFCALC = .TRUE. ; AEXX = 1.0 ; ALDAC = 0.0 ; AGGAC = 0

†A. V. Krukau , O. A. Vydrov, A. F. Izmaylov, and G. E. Scuseria, J. Chem. Phys. **125**, 224106 (2006).

Band structure with VASP

(A) Standard procedure (DFT)

① Create SC charge density (CHGCAR) using a uniform k-point mesh (for instance 8x8x8)
② Perform a non-SC calculation (ICHARG=11) using the pre-converged charge density (CHGCAR) from step 1, and a new KPOINTS file with the suitable high-symmetry k-points and number of intersections.

KPOINTS

```
10 k-points along G-X
10 ! 10 intersections
Line-mode
cart
0 0 0 ! G
0 0 1 ! X
```

③ plot with p4v

Band structure with VASP

(B) Additional zero-weight **k**-points procedure (HF)

① Standard HF/DFT+HF using a conventional (uniform) k-point mesh
② (i) cp IBZKPT KPOINTS (explicit list of k-points used in step (1)
(ii) add desired k-points with zero weight:

KPOINTS

```
Automatically generated mesh
18
Reciprocal lattice
 0.00000000000000  0.00000000000000  0.00000000000000 1
 0.25000000000000  0.00000000000000  0.00000000000000 8
 0.50000000000000  0.00000000000000  0.00000000000000 4
 0.25000000000000  0.25000000000000  0.00000000000000 6
 0.50000000000000  0.25000000000000  0.00000000000000 24
-0.25000000000000  0.25000000000000  0.00000000000000 12
 0.50000000000000  0.50000000000000  0.00000000000000 3
-0.25000000000000  0.50000000000000  0.25000000000000 6
 0.00000000 0.00000000 0.00000000 0.000
 0.00000000 0.05555556 0.05555556 0.000
 0.00000000 0.11111111 0.11111111 0.000
 0.00000000 0.16666667 0.16666667 0.000
 0.00000000 0.22222222 0.22222222 0.000
 0.00000000 0.27777778 0.27777778 0.000
 0.00000000 0.33333333 0.33333333 0.000
 0.00000000 0.38888889 0.38888889 0.000
 0.00000000 0.44444444 0.44444444 0.000
 0.00000000 0.50000000 0.50000000 0.000
```

③ Plot with p4v (remove **k**-points of uniform mesh)

Band structure with VASP

(C) Interpolation using MLWFs via VASP2WANNIER90 (DFT, HF, DFT+HF, GW)

① Standard DFT calculation using a conventional (uniform) k-point mesh. Include TAG LWANNIER90=.TRUE. to generate a default wannier90.win file.

② Suitably modify wannier90.win according to the instructions given in the WANNIER90 manual, and run VASP again (DFT/HF/HF+DFT/GW) in order to generate the inputs file for the wannier90 interpolation (wannier90.eig, wannier90.amn, wannier90.mmn)

③ Run WANNIER90 (wannier90.x wannier90) in order to generate the MLWFs. Input files: wannier90.win, wannier90.eig, wannier90.amn, and wannier90.mmn.

④ Run WANNIER90 in Band structure mode (add band structure flags in wannier90.win). Input files: wannier90.win, wannier90.chk, and wannier90.eig.

⑤ Plot using xmgrace or gnuplot.

(Compile with -DVASP2WANNIER90, see http://cms.mpi.univie.ac.at/wiki/index.php/LWANNIER90)

VASP2WANNIER90:

C. Franchini, R. Kovácik, M. Marsman, S.S. Murthy, J. He, C. Ederer, G. Kresse, J. Phys.: Condens. Matter **24**, 235602 (2012).

Wannier90.win for Si

```
num_wann=8
num_bands=8
Begin Projections
Si:sp3
End Projections
dis_froz_max=9
dis_num_iter=1000
guiding_centres=true
# BS flags restart = plot
bands_plot = true
begin kpoint_path
G 0.00000 0.00000 0.0000 X 0.50000 0.00000 0.5000
end kpoint_path
bands_num_points 40
bands_plot_format gnuplot xmgrace
begin unit_cell_cart
2.7150000 2.7150000 0.0000000
0.0000000 2.7150000 2.7150000
2.7150000 0.0000000 2.7150000
end unit_cell_cart
begin atoms_cart
Si 0.0000000 0.0000000 0.0000000
Si 1.3575000 1.3575000 1.3575000
end atoms_cart
mp_grid = 4 4 4
begin kpoints
0.0000000 0.0000000 0.0000000
0.2500000 0.0000000 0.0000000
...
-0.2500000 0.2500000 -0.5000000
end kpoints
```

Return to direct optimization: Why?

Pure DFT functionals depend only in the density

$$\left(1 - \sum_m |\psi_m\rangle\langle\psi_m|\right) \hat{H}|\psi_n\rangle$$

DFT-Hartree-Fock hybrid functionals depend explicitly on the orbitals

$$\left(-\frac{1}{2}\Delta + V_{\text{eff}}[\rho](\mathbf{r}) + V_{\text{ext}}(\mathbf{r})\right)\psi_n(\mathbf{r}) + C\sum_m^{\text{occ}} \psi_m(\mathbf{r}) \int \frac{\psi_m^*(\mathbf{r}')\psi_n(\mathbf{r}')}{|\mathbf{r}-\mathbf{r}'|} d\mathbf{r}' = \epsilon_n \psi_n(\mathbf{r})$$

So density-mixing will not always work (reliably).

Unfortunately we know direct optimization schemes are prone to charge sloshing for metallic and small-gap systems.

Mixed scheme

- The gradient of the wave functions is given by

$$|g_n\rangle = f_n\left(1 - \sum_m |\psi_m\rangle\langle\psi_m|\right)\hat{H}|\psi_n\rangle + \sum_m \frac{1}{2}\mathbf{H}_{nm}(f_n - f_m)|\psi_m\rangle$$

where

$$\mathbf{H}_{nm} = \langle\psi_m|\hat{H}|\psi_n\rangle$$

- A search direction towards the groundstate w.r.t. unitary transformations between the orbitals within the subspace spanned by the orbitals can be found from perturbation theory:

$$\mathbf{U}_{nm} = \delta_{nm} - \Delta s \frac{\mathbf{H}_{nm}}{\mathbf{H}_{mm} - \mathbf{H}_{nn}}$$

But this is exactly the term that is prone to charge sloshing!

- Solution: Use density mixing to determine the optimal unitary transformation matrix $\mathbf{U}_{nm}$.

Optimal subspace rotation

- Define a Hamilton matrix: $\bar{\mathbf{H}}_{kl} = \langle\psi_l|\bar{H}[\rho]|\psi_k\rangle$

  where $\bar{H}[\rho] = \hat{T} + \hat{V}_{\rm ext} + \hat{V}_{\rm eff}[\rho] + \hat{V}_{\rm X}^{\rm nl}[\{\psi\},\{f\}]$

- Determine the subspace rotation matrix **V** that diagonalizes the Hamiltonian.
- Recompute the (partial) occupancies ⟶ {f'}
- The transformed orbitals:

$$\sum_l \mathbf{V}_{nl}\psi_l$$

  and partial occupancies {f'} define a new charge density ρ'

- Mix ρ and ρ'
- and iterate the above until a stable point is found ⟶ ρ_{sc}
- The optimal subspace rotation is then given by :

$$\mathbf{U}_{nm} = \delta_{nm} - \Delta s \frac{\mathbf{H}^{\rm sc}_{nm}}{\mathbf{H}^{\rm sc}_{mm} - \mathbf{H}^{\rm sc}_{nn}}$$

  where

$$\mathbf{H}^{\rm sc}_{nm} = \langle\psi_m|\bar{H}[\rho_{\rm sc}]|\psi_n\rangle$$

- N.B.: we do not update the orbital dependent part of the Hamiltonian $\hat{V}_{\rm X}^{\rm nl}[\{\psi\},\{f\}]$

The full mixed scheme

The iterative optimization of the orbitals cycles through the following steps:

1. Construct the Hamiltonian **H**, from the current orbitals and partial occupancies, and calculate $\mathbf{H}|\boldsymbol{\psi}\rangle$

2. Inner loop: determine the self-consistent Hamiltonian $\mathbf{H}^{sc}$, defining the preconditioned direction for the optimal subspace rotation **U**.

3. Minimization along the preconditioned search direction defined by

$$\left(1 - \sum_m |\psi_m\rangle\langle\psi_m|\right) \hat{H}|\psi_n\rangle$$

   and by **U**, and by a gradient acting on the partial occupancies.
   For instance by means of a conjugate-gradient algorithm.

This loop is repeated until the change in the free energy from one iteration to the next drops below the required convergence threshold ΔE_{thr} (usually 10^{-4} eV).

Example: fcc Fe

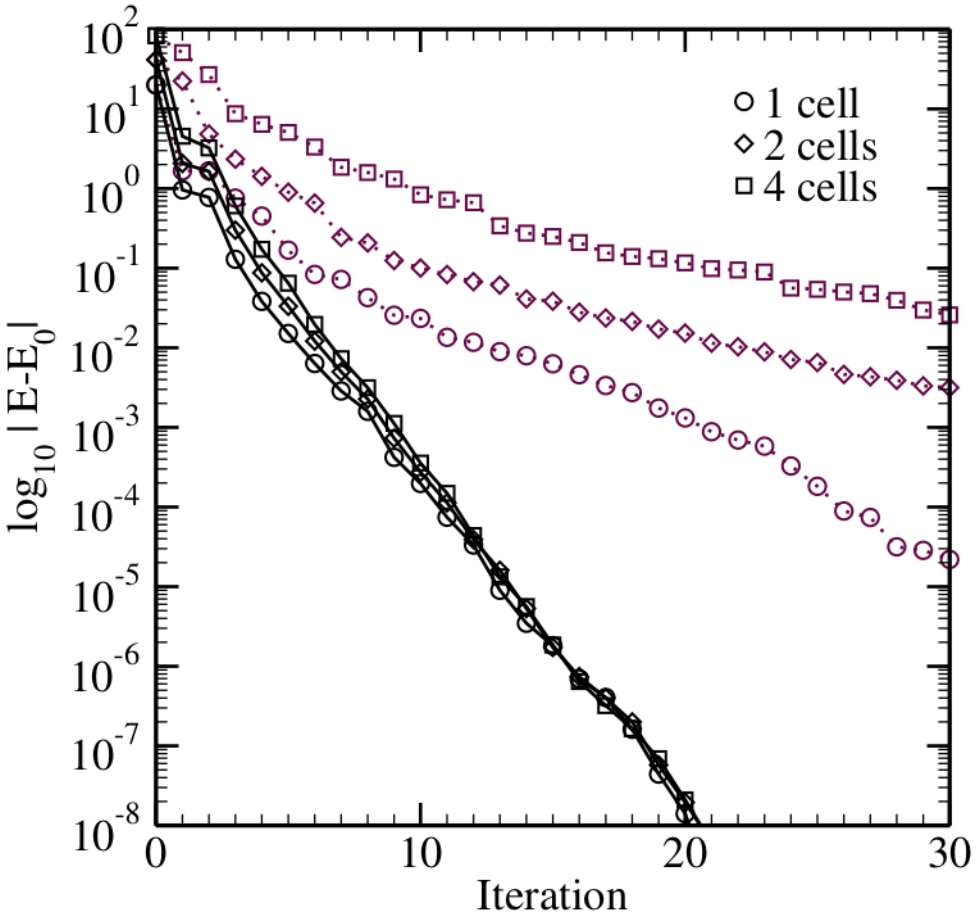

The convergence behaviour of HSE03 calculations using the improved direct optimization procedure (solid lines) and a standard conjugate gradient algorithm (dotted lines). Calculations on single, double, four times repeated cells are marked with circles, diamonds, and squares, respectively.

INCAR Tags and links

ALGO The INCAR tag that sets which algorithm is used for the electronic minimization.

IALGO and LDIAG Same as above, but more to choose from (ALGO is the preferred tag). For the direct optimizers (ALGO =All | Damped) LDIAG = .TRUE. switches on the density mixer in the determination of the subspace rotation matrix.

Mixing tags The VASP manual chapter on the settings for the density mixer.

TIME Time step in the direct optimization method ALGO = Damped, and trial time step for the conjugate gradient direct optimizer ALGO = All.

Electronic optimization Lecture from the VASP workshop in Vienna (2003).

Hartree-Fock within the PAW formalism

In principle we would want to follow the original scheme:

- Solve the non-spinpolarized spherical atom within the (scalar relativistic) Hartree-Fock approximation.
- Compute all-electron partial waves.
- Pseudize .. etc etc …

Unfortunately this is altready problematic in the second step, solving

$$(-\frac{1}{2}\Delta + v_H + \hat{v}_X)|\phi_i\rangle = \epsilon_i|\phi_i\rangle$$

with

$$\langle r|\hat{v}_X|\phi_i\rangle \propto \sum_a^{\text{at.ref}} \phi_a(\mathbf{r}) \int \frac{\phi_a^*(\mathbf{r}')\phi_i(\mathbf{r}')}{|\mathbf{r}-\mathbf{r}'|} d\mathbf{r}'$$

$\Longrightarrow$ numerically unstable for unbound partial waves with $\epsilon < 0$.

The HF-PAW method (cont.)

A pragmatic solution:

- Keep the partial waves and projector functions ($|\phi_i\rangle$, $|\tilde{\phi}_i\rangle$, and $|\tilde{p}_i\rangle$) obtained with DFT.
- Orthogonalize the all-electron partial waves $|\phi_i\rangle$ with respect to the Hartree-Fock core states $|\phi_i\rangle \rightarrow |\phi'_i\rangle$.
- Compute the PAW strength parameters and augmentation charges using $|\phi_i\rangle$ and the Hartree-Fock core states:

$$D_{ij} = \langle\phi'_i| - \frac{1}{2}\Delta + v_H^1[\rho_v^1] + v_H^1[\rho_{Zc}^{\mathrm{HF}}] + v_X^1[\{\rho_{ij}\}] + v_X^{\mathrm{c-v}}[\{\phi_c^{\mathrm{HF}}\}]|\phi'_j\rangle$$
$$- \langle\tilde{\phi}_i| - \frac{1}{2}\Delta + v_H^1[\tilde{\rho}_v^1] + v_H^1[\tilde{\rho}_{Zc}] + \tilde{v}_X^1[\{\rho_{ij}\}]|\tilde{\phi}_j\rangle$$

and

$$Q_{ij} = \langle\phi'_i|\phi'_j\rangle - \langle\tilde{\phi}_i|\tilde{\phi}_j\rangle$$

The most important step in this scheme is: $v_H^1[\rho_{Zc}^{\mathrm{DFT}}] \rightarrow v_H^1[\rho_{Zc}^{\mathrm{HF}}]$

The HF-PAW method (cont.)

Bulk equilibrium volumes for GaAs and Si:

Valence electrons Ga	Valence electrons As	GaAs: Ω_0 (Å^3) PAW	GaAs: Ω_0 (Å^3) HF-PAW
$4s^2 4p^1$	$4s^2 4p^3$	46.06	48.79
$3d^{10} 4s^2 4p^1$	$4s^2 4p^3$	47.07	47.80
$3p^6 3d^{10} 4s^2 4p^1$	$3d^{10} 4s^2 4p^3$	47.74	47.80

Valence electrons Si	Si: Ω_0 (Å^3) PAW	Si: Ω_0 (Å^3) HF-PAW
$3s^2 3p^2$	41.44	41.86
$2s^2 2p^6 3s^2 3p^2$	41.91	41.93

3s and 3p levels in the spherical Si atom.

	$3s^2 3p^2$		$2s^2 2p^6 3s^2 3p^2$		HF ref.
	PAW	HF-PAW	PAW	HF-PAW	
$3s$	-15.967	-15.918	-15.895	-15.908	-15.906
$3p$	-2.761	-2.756	-2.749	-2.756	-2.760
Δ	-13.205	-13.161	-13.146	-13.151	-13.147

All energies in eV.

The HF-PAW method (cont.)

The remaining discrepancies are related to the fact that the one-center expansions of the wave functions inside the PAW spheres are not complete enough (particularly further away from the nucleus)

$$\psi_n(\mathbf{r}) \neq \sum_i \phi_i(\mathbf{r})\langle \widetilde{p}_i|\widetilde{\psi}_n\rangle \qquad \widetilde{\psi}_n(\mathbf{r}) \neq \sum_i \widetilde{\phi}_i(\mathbf{r})\langle \widetilde{p}_i|\widetilde{\psi}_n\rangle$$

This causes problems for at least two reasons:

1. The core-valence exchange interaction is computed between the Hartree-Fock core states $\{\psi_c^{\mathrm{HF}}\}$ and the one-center expansion of ψ only.

2. The point where the Hartree potentials arising from the all-electron and pseudo ionic cores match moves into regions where the one-center expansions are not good. This is bound to happen to some degree since we adjust:

$$v_H^1[\rho_{Zc}^{\mathrm{DFT}}] \rightarrow v_H^1[\rho_{Zc}^{\mathrm{HF}}]$$

and leave $v_H^1[\widetilde{\rho}_{Zc}]$ fixed.

The HF-PAW method (cont.)

$$|\widetilde{\psi}_n(\mathbf{r})|^2 \neq \sum_{ij} \langle \widetilde{\psi}_n | \widetilde{p}_i \rangle \langle \widetilde{\phi}_i | \mathbf{r} \rangle \langle \mathbf{r} | \widetilde{\phi}_j \rangle \langle \widetilde{p}_j | \widetilde{\psi}_n \rangle$$

$$\widetilde{\rho} \neq \widetilde{\rho}^1$$

$$\sum_{ij} \langle \widetilde{\psi}_n | \widetilde{p}_i \rangle \langle \phi_i | \mathbf{r} \rangle \langle \mathbf{r} | \phi_j \rangle \langle \widetilde{p}_j | \widetilde{\psi}_n \rangle \neq |\phi^{\mathrm{ref}}_{\mathrm{HF}}(\mathbf{r})|^2$$

$$\rho^1 \neq \rho^1_{\mathrm{HF}}$$

$$\widetilde{\rho} - \widetilde{\rho}^1 + \rho^1 \approx \rho^1_{\mathrm{HF}}$$

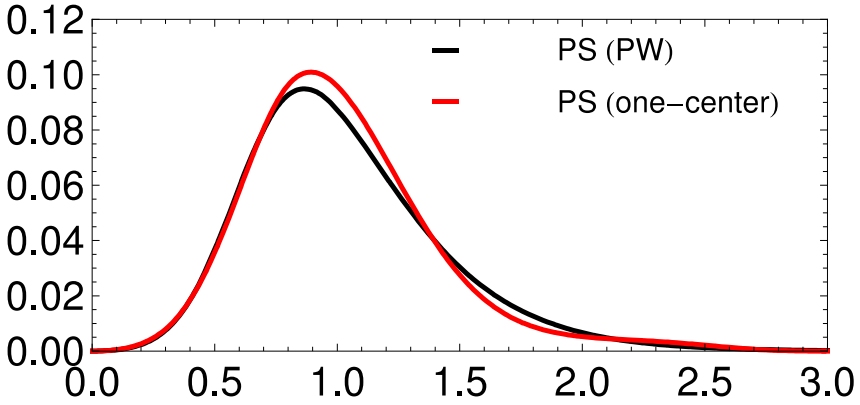

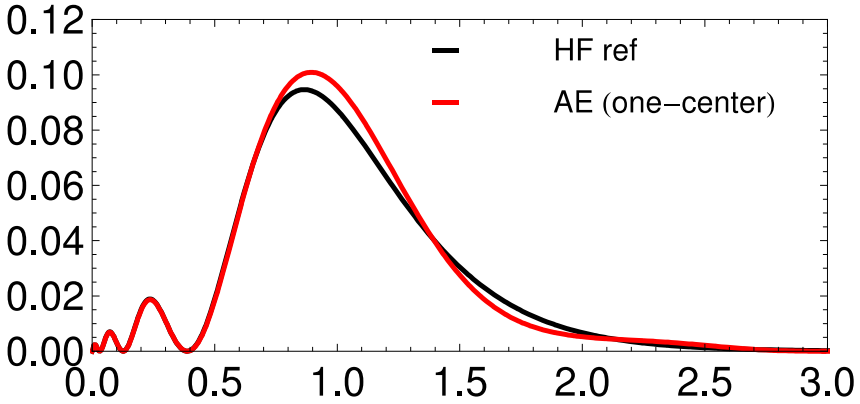

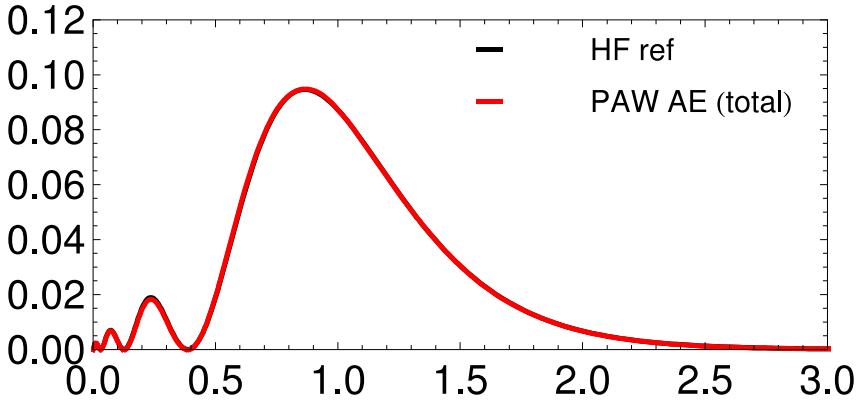

INCAR Tags and links

LRHFATM = .TRUE.

Changes the DFT AE core charge density (ρ^1) to a Hartree-Fock one.

The End

Thank you!